P1.1 A SEQUENTIAL ESTIMATOR FOR ASSIMILATION OF GROUND- AND SPACE-BASED MESOSPHERIC AND LOWER THERMOSPHERIC WINDS

R. S. Lieberman* and D. M. Riggin
Northwest Research Associates
Colorado Research Associates Division
Boulder, CO

R. R. Garcia
National Center for Atmospheric Research
Boulder, CO

1 INTRODUCTION

The mesosphere and lower thermosphere (MLT) are regions that absorb and modify atmospheric phenomena originating in the troposphere and stratosphere. However, these are also source regions for dynamical, chemical and radiative processes that act to redistribute energy, momentum and constituents throughout the upper atmosphere. The specification of MLT dynamics is critical for successful physics-based modeling of the neutral atmosphere, and its links to the thermosphere. The MLT is monitored by the Upper Atmosphere Research Satellite (UARS) and the Thermosphere-Ionosphere-Mesosphere Dynamics and Energetics (TIMED) spacecraft, and ground-based networks of lidars, optical sensors, and wind radars. In support of the TIMED mission science goals and their application to the Space Weather Program, we have developed a sequential estimator for the assimilation of ground- and satellite-based MLT wind measurements.

The present report focuses on the capabilities of a sequential estimator to retrieve the daily evolution of diurnal tides sampled by the TIMED Doppler Interferometer (TIDI), and by ground-based wind radars. Diurnal tides comprise a very significant component of the planetary-scale zonal and meridional wind fields at low and subtropical latitudes. These oscillations contribute to the westward momentum budget of the tropical MLT, and modulate the transmission, dissipation, and momentum deposition by gravity waves. Recent studies have highlighted temporal variability in diurnal tides that may be linked to interactions with planetary waves (Teitelbaum and Vial, 1991; Pancheva et al., 2002; Angelats i Coll and Forbes, 2002; Lieberman et al., 2003). The products of the sequential estimator, daily tidal coefficients, are key to our research goals of clarifying the role of planetary waves for tidal variability.

2 BRIEF OVERVIEW OF SEQUENTIAL ESTIMATION

The method of sequential estimation generates a series of minimum-variance estimates. Given an estimate X_e with a variance of σ_e and a measurement X_i whose variance is σ_i, the optimal (or minimum-variance) combination of these two data is given by

$$\widehat{X} = \widehat{\sigma}^2 \left[\frac{X_i}{\sigma_i^2} + \frac{X_e}{\sigma_e^2} \right] \quad (1)$$

$$\widehat{\sigma}^2 = \left[\frac{1}{\sigma_i^2} + \frac{1}{\sigma_e^2} \right]^{-1} \quad (2)$$

Note that the variance of the optimal combination is lower than the uncertainties of the measurement and the estimate. Equation (1) is applied sequentially to a "virtual" dataset (described in section 3) at longitudes and universal times corresponding to TIMED (satellite) and MF sampling.

Planetary-scale atmospheric phenomena are generally represented as Fourier series of zonal wavenumbers. Our studies to date have focused on tidal meridional wind

*Corresponding author address: Ruth S. Lieberman, Colorado Research Associates, 3380 Mitchell Lane, Boulder, CO 80301; e-mail: ruth@colorado-research.com.

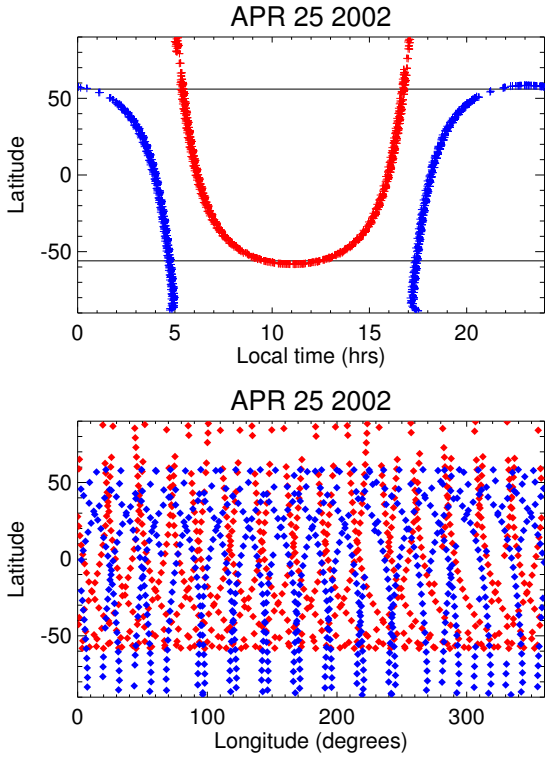

Figure 1: Top: Latitude versus local time of TIDI measurements in the 80–105 km altitude range on April 25, 2002. Red (blue) symbols denote warm- (cold-) sided viewing. Bottom: Corresponding latitudes versus longitudes.

definitions, approximated as

$$V(\lambda_i, t_0) = \sum_{m=-6}^{6} A_{m,1}(t_0)\cos(m\lambda_i + \Omega t) \quad (3)$$

$$+B_{m,1}(t_0)\sin(m\lambda_i + \Omega t) \quad (4)$$

Thus, the products of the sequential estimator are daily diurnal ($A_{m,1}$ and $B_{m,1}$) coefficients for the zonal mean, and 6 eastward and westward-propagating zonal wavenumbers. It can be shown that the optimum estimate $\widehat{V}$ and its variance $\widehat{\sigma}$ at the ith time step are given by

$$\widehat{V}_i = V_e + \frac{(V_i - V_e)\sigma_e^2}{\sigma_e^2 + \sigma_i^2}, \quad (5)$$

$$\widehat{\sigma}_i^{-2} = \sigma_i^{-2} + \sigma_e^{-2} \quad (6)$$

(Khouri, 1981; Haggard et al., 1986).

Equation (3) tells us that $\widehat{V}_i$ is a linear combination of the actual measurement V_i and the Fourier series approximation to V given by equation (2), denoted V_e. The weighting of V_e and V_i depends upon the ratio of the measurement uncertainty σ_i to the estimate uncertainty σ_e. If high-quality (low variance) data are available, the measurement is weighted more heavily than the Fourier estimate. Conversely, if the data are very noisy (large σ_i^2), $\widehat{\sigma}_i = \sigma_e$, and $\widehat{V}_i = V_e$. In this case, the Fourier coefficients determined at the previous time step are not updated, and the optimum estimate $\widehat{V}_i$ is based entirely upon the Fourier approximation given by equation (2).

3 VIRTUAL DATASET

The TIMED spacecraft was launched successfully in December 2001 with the mission of determining MLT waves, basic states, and energy balance. The wind-measuring instrument, TIDI, senses emissions on both the dayside and the nightside between 80 and 105 km and 60S-60N. Each day's worth of TIDI measurements occur in 4 sets of 15 "swaths" (Figure 1b). The satellite precesses about 24° in longitude between each swath; however, at a given latitude, the local time associated with a particular swath is nearly invariant over the course of one day (Figure 1a). MLT winds are also sampled by a global network of meteor and medium frequency (MF) radars. These instruments provide virtually continuous measurements in time.

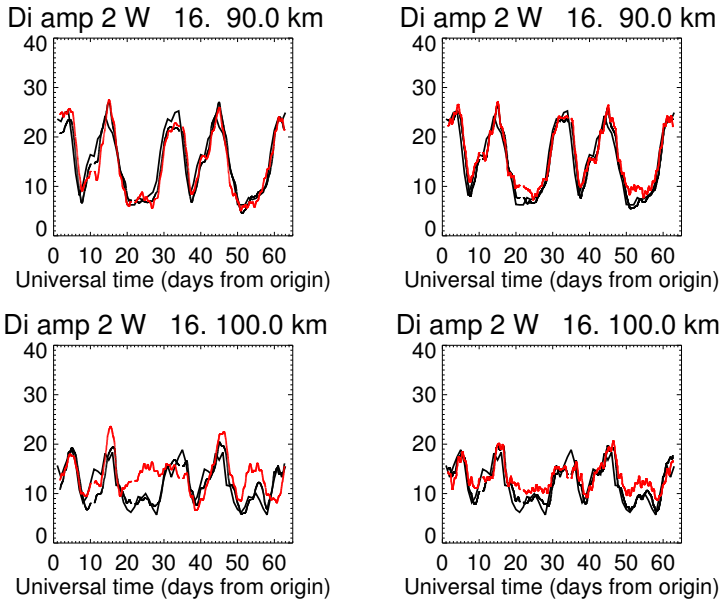

Figure 2: Amplitude of the diurnal westward wavenumber 2 component (W2), as a function of time at 16°N at 90 km (top) and 100 km (bottom). Thick solid curve is the variation of W2 within WACCM, thin curves are W2 retrievals of WACCM fields using sequential estimation. Left-side plots show results for WACCM sampling by TIDI only, right-side plots show results for WACCM sampled by TIDI and 7 MF radars sampling every 4 hours, and equispaced in longitude. Thin red lines are W2 retrievals using a sequential estimator applied to the complete WACCM spectrum. Thin black lines are W2 retrievals when WACCM spectrum is truncated at 1.8 days. All time series are smoothed with a 3-day running mean.

In order to assess the efficacy of the sequential estimator, we examine meridional wind "data" from a 30-day March "run" of the NCAR Whole Atmosphere Community Climate Model (WACCM). The full range of temporal variability in the WACCM field extends from the Nyquist period (6 hours) to the fundamental period (30 days). WACCM spectra were used to reconstruct the evolution of the meridional wind field at TIDI and MF radar longitudes and universal times, throughout a full 64-day TIMED "yaw" period extending from March 19–May 22, 2002. The sequential estimator was operated on the time series in both forward and backward directions; forward and backward estimates are then optimally combined to yield a final minimum variance estimate at each time step. The output of the sequential estimator consists of daily zonal wavenumber coefficients of diurnal waves 0–6.

Instrument errors and geophysical variances for diurnal zonal wavenumbers 0–6 are required for the construction of the sequential estimator. For our experiments, all measurement variances are set to 4 m^2 s^{-2}, while the geophysical variances of wavenumbers 0–6 are uniformly set to 200 m^2 s^{-2}. Wave coefficients were initialized to zero for the forward "run". Their values at the final timestep of the forward run are used as the initial values input to the backward run.

4 RESULTS

We examine first the evolution of a nonmigrating diurnal tide, the westward-propagating wavenumber 2 diurnal tide (denoted W2). This mode was chosen because of a striking 10–20-day amplitude modulation that is evident at 90 km (Figure 2, top). The sequential estimator retrieves this mode with very good accuracy at 90 km. At 100 km, however, the retrieval that is based upon satellite data alone (lower left panel) is not as accurate as its 90 km counterpart. The poorer performance at 100 km is due to aliasing by semidiurnal tides, which are not fully resolved by TIDI's sampling. This can be seen by comparing the thin red and black curves in Figure 2. When WACCM fields are filtered of semidiurnal variability, diurnal definitions provided by the sequential estimator (thin black curves) are in better

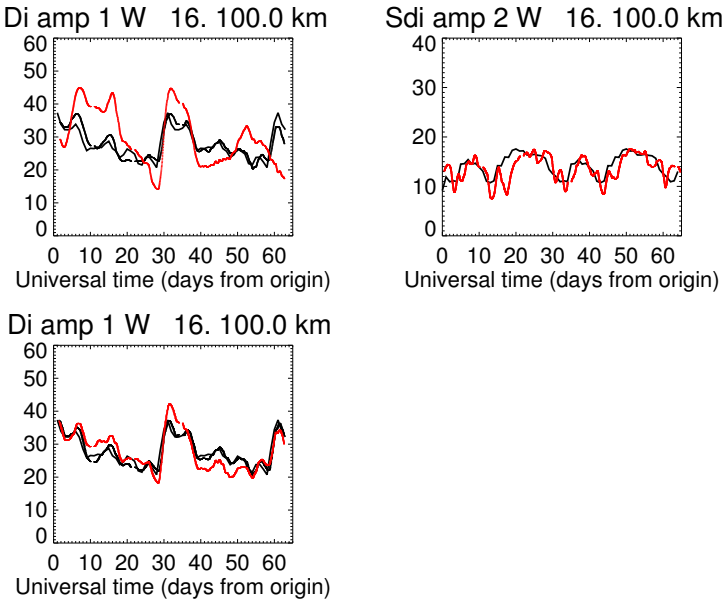

Figure 3: Left: Amplitude of the migrating diurnal tide (westward wavenumber 1 component, or W1) at 16°N at 100 km. Thick solid line is the variation of W1 within WACCM, thin lines are W1 retrievals of WACCM fields using sequential estimation. Top left plot shows results for WACCM sampling by TIDI only, bottom left show results for WACCM sampled by TIDI and 7 MF radars sampling every 4 hours, and equispaced in longitude. Thin red lines are W1 retrievals using a sequential estimator applied to the complete WACCM spectrum. Thin black lines are W1 retrievals when WACCM spectrum is truncated at 1.8 days. Right hand plot shows the amplitude of the migrating semidiurnal tide (westward wave 2), retrieved by a sequential estimator with WACCM input sampled by TIDI and 7 equispaced MF radars sampling every 4 hours. All time series are smoothed with a 3-day running mean.

agreement with WACCM.

In order to retrieve day-to-day evolution of tidal variations at altitudes where the semidiurnal tides are comparable to the diurnal tide, the sampling rate must be increased above the 4 local times per day provided by TIDI. Moreover, higher sampling rates in local time must exist at sufficient longitudes to resolve the strongest planetary-scale semidiurnal modes. When the sequential estimator is applied to an observational network consisting of TIDI, and 7 ground-based MLT wind platforms equispaced in longitude, agreement between the retrieved and WACCM tidal input is substantially improved. Figure 2 (bottom right) illustrates the effects of additional ground-based sampling for diurnal W2, while Figure 3 (left side) demonstrates the effect of sampling upon the migrating diurnal (W1) component.

We have applied a sequential estimator based upon the inclusion of semidiurnal tides in the Fourier representation. For this version, equation (1) is modified to

$$V(\lambda_i,t_0) = \sum_{m=0}^{M-1} A_{m,1}(t_0)\cos(m\lambda_i+\Omega t) + B_{m,1}(t_0)\sin(m\lambda_i+\Omega t) + \sum_{m=2}^{2} A_{m,2}(t_0)\cos(m\lambda_i+2\Omega t) + B_{m,2}(t_0)\sin(m\lambda_i+2\Omega t) \quad (7)$$

A retrieval of the migrating semidiurnal tide is shown in Figure 3 (top right), using a sequential estimator based upon (4) and applied to WACCM winds sampled by TIDI and by 7 ground-based wind stations.

Figures 2 and 3 clearly illustrate the dependence of diurnal and semidiurnal retrievals upon their relative magnitudes, and the combination of TIDI and ground-based sampling. These effects are summarized in Figure 4. Diurnal and semidiurnal amplitude spectra from WACCM are shown, together with the root-mean-squared (RMS) errors of their estimates provided by the sequential estimator. We note two features in these plots. First, errors generally decrease as the number of ground-based stations is increased. In the case of the diurnal tides, a sharp drop-off in RMS error magnitudes occurs when the 5th radar is added to the database. Second, the error-to-amplitude ra-

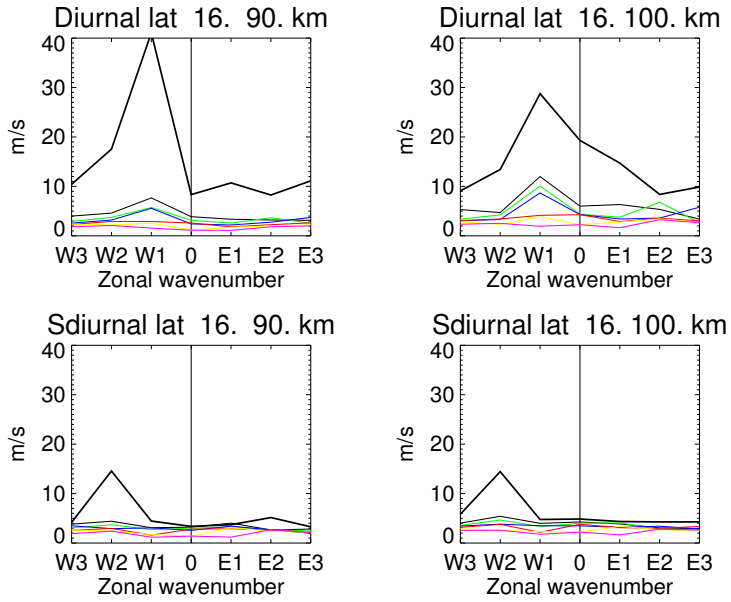

Figure 4: Amplitude WACCM diurnal (top) and semidiurnal (bottom) tides as a function of zonal wavenumber, plotted as heavy solid black curves. Left-side plots are for 90 km, right side plots are results at 100 km. Thin curves are RMS errors for sequential estimator retrievals based upon combined TIDI and 4-hourly, longitudinally equispaced radar sampling according to the following color index: Black: 2 radars. Green: 3 radars. Blue: 4 radars. Red: 5 radars. Yellow: 6 radars. Magenta: 7 radars.

tios for the migrating diurnal tide are smaller, and drop off more rapidly with respect to number of ground radar sites when the diurnal amplitude exceeds the semidiurnal amplitude by a factor of more than 2. At 90 km, where the migrating diurnal amplitude exceeds 40 m s^{-1}, the corresponding RMS error does not exceed 8 m s^{-1}, or 20% of the amplitude. At 100 km, the migrating diurnal amplitude is reduced to 29 m s^{-1}, compared to an amplitude of 15 m s^{-1} for the migrating semidiurnal tide. The corresponding RMS errors range between 8 and 12 m s^{-1} with the inclusion of 4 and 2 radars, respectively. This demonstrates that assimilation is more difficult when diurnal and semidiurnal tides have comparable amplitudes.

5 SUMMARY

We have developed a sequential estimator that provides daily tidal definitions using TIDI and ground-based neutral winds. This project is motivated in part by reports of tidal variability on timescales matching periods of planetary waves. Experiments with the sequential estimator indicate that at tropical latitudes, and up to 90 km, diurnal planetary-scale waves are well-retrieved when sampled at 4 local times daily by TIDI. However, at midlatitudes, and above 95 km, TIDI sampling must be augmented in local time with ground-based radar winds in order to carry out tidal retrievals. Accuracy of the sequential estimator is enhanced when ground-based wind data sampled at a minimum of 5 local times per day are added to the TIDI-sampled database. The enhancements are most significant when ground-based stations are equispaced in longitude, and exceed 4 in number. These requirements arise from the presence of the semidiurnal tide, which contaminates diurnal retrievals based on data sampled fewer than 5 times per day.

6 References

Angelats i Coll, M. and J. M. Forbes, 2002: Nonlinear interactions in the upper atmosphere: The s 1 and s 3 nonmigrating semidiurnal tides. J. Geophys. Res., 107, SIA 3 1 3 15.

Haggard, K. V., E. E. Remsberg, W. L. Grose, J. M. Russell, B. T. Marshall, and G. Lingenfelser, 1986: Descrip-

tion of data on Nimbus 7 LIMS map archive tape. Technical Report 2553, 1 52. NASA technical paper.

Khouri, W. J., 1981: LRIR observations of the structure and propagation of the stationary planetary waves in the Northern hemisphere during December 1975. Technical Report NCAR/CT-63, 1 312. Available from NTIS as PB82 156 639.

Lieberman, R. S., J. Oberheide, M. E. Hagan, E. E. Remsberg, and L. L. Gordley, 2003: Variability of diurnal tides and planetary waves during November 1978 May 1979. J. Atmos. Sol.-Terr. Phys. To Appear.

Pancheva, D., E. Merzylyakov, N. J. Mitchell, Y. Portnyagin, A. H. Manson, C. Jacobi, C. E. Meek, Y. Luo, R. R. Clark, W. K. Hocking, J. MacDougall, H. G. Muller, D. Kurschner, G. O. L. Jones, R. A. Vincent, I. M. Reid, W. Singer, K. Igarashi, G. I. Fraser, et al., 2002: Global-scale tidal variability during the 8 PSMOS campaign of June August 1999; interaction with planetary waves. J. Atmos. Sol.-Terr. Phys., 64, 1865 1896.

Teitelbaum, H. and F. Vial, 1991: On tidal variability induced by nonlinear interaction with planetary waves. J. Geophys. Res., 96, 14,169 14,178.

Acknowledgements

This work was supported by the National Science Foundation under grant number NSF-0228289.